Journal of Thermal Analysis and Calorimetry, Vol. 83 (2006) 2, 415–419

TIME AND TEMPERATURE-BASED STUDY FOR THE PRODUCTION OF HIGH T_C PHASE BY SOL–GEL TECHNIQUE IN Pb–BSCCO SYSTEM

M. Arshad[1*] *and A. H. Qureshi*[2]

[1]APD, PINSTECH, P.O. Nilore, Islamabad, Pakistan
[2]NMD, PINSTECH, P.O. Nilore, Islamabad, Pakistan

The high T_C superconducting phase $Bi_2Sr_2Ca_2Cu_3O_x$ (2223) in the Pb–BSCCO system has been produced by EDTA-gel processing using nitrate solutions. The precursor has heated in two stages, at 300 and 800°C each for 2 h, to avoid the burning of the important species involved in the final product. The effects of time (6 to 48 h) and temperature (845 and 855°C) on the formation of the 2223 phase have been studied by sintering the samples in air. Thermal analysis (TG/DTA), X-ray diffraction (XRD), scanning electron microscopy (SEM) and a vibrating sample magnetometer (VSM) have been employed to investigate the powder produced at different stages of decomposition, oxidation and formation of sintered materials from the powders. The volume-fraction of the 2223 phase at 845°C increases with time, the maximum value of the 2223 phase was obtained at 120 h. It has been observed that the formation of the high T_C phase is remarkably enhanced at the temperature of the endothermic peak of the DTA curve. The best result has been obtained in the sample sintered for 24 h at the temperature 855°C (endothermic peak). This also indicated that at 855°C, the large volume-fraction of 2223 phase with T_C 113 K grew in short time and as the sintering time increased, it decomposed into the $Bi_2Sr_2CaCu_2O_x$ (2212) phase and other phases.

Keywords: *annealing effect, high T_C phase, Pb–BSCCO system, superconducting phase, thermal analysis, XRD study*

Introduction

The production of superconducting phases and others by sol–gel technique and their characterization by thermal and spectroscopic techniques have been the subject of a number of communications [1-8]. Many researchers have reported [9–11] that a large volume-fraction of the 2223 phase in the Bi–Sr–Ca–Cu–O (BSCCO) system can be prepared with the partial substitution of Pb for Bi.

In addition to chemical composition, the time, the temperature and the other sintering conditions also play important roles in obtaining the high volume-fraction of high T_C phase in BSCCO and Pb–BSCCO systems. Hatano *et al.* [12] noticed that the volume-fraction of the 2223 phase in BSCCO and Pb–BSCCO systems can be enhanced by sintering the material at the temperature of the endothermic peak. From the processing point of view, it has been reported [13–15] that the sol-gel technique obviates several cycles of firing and grinding of oxides or carbonates, which are required in conventional processing. In the present work the use of ethylenediaminetetraacetic acid (EDTA) as the organic complexing agent for gel formation with Pb addition in BSCCO system has been investigated. We have reported results attained for the sample $Bi_{1.6}Pb_{0.4}Sr_2Ca_2Cu_4O_x$ as a function of Pb substitution and sintering temperature determined from DTA curve.

Experimental

The individual solution containing 'Analar Grade' EDTA and nitrates of Bi, Pb, Sr, Ca and Cu were mixed together in the required compositions to produce solution for gel production. Powder mixture of the nominal composition $Bi_{1.6}Pb_{0.4}Sr_2Ca_2Cu_4O_x$ was prepared. The individual nitrate solutions were mixed together and the desired EDTA solution was gradually added to the nitrate solution. The pH of the solution was maintained between 5 and 6 using ammonia. The mixed solution was concentrated using a rotary evaporator, which was maintained at 80°C under vacuum until a viscous liquid was obtained. The liquid was placed in an evaporating dish and was left in a vacuum oven at 80°C for 24 h in order to produce the dried precursor. The batches of precursor were fired in a muffle furnace at 300°C in air for 2 h prior to a higher temperature firing at 800°C to get oxide powder. To monitor the formation of the different phases, the pellets of oxide powder were sintered in a tube furnace in air. The thermal stability of the precursor and its decomposition products were studied by using a Seiko Simultaneous Thermal Analyser 429 with heating rate of 10°C min^{-1} under a 100 mL min^{-1} flow rate of air over the temperature range of ambient to 900°C. X-ray diffraction (XRD) analysis of the products was carried out using CuK_α radiation and a

---

[*] Author for correspondence: marshads53@yahoo.com.sg

1388–6150/$20.00

Akadémiai Kiadó, Budapest, Hungary
Springer, Dordrecht, The Netherlands

Philips diffractometer with a voltage of 40 kV and a current of 20 mA. Microstructures of the fractured specimens were studied using a Philips 505 SEM. The AC magnetic susceptibility of the samples was measured with an Oxford Instruments vibrating sample magnetometer (VSM). The energy dispersive X-ray (EDX) microanalysis of the plate-like grains was carried out using Philips 505 SEM equipped with an EDX 9100/60 detector.

Results and discussion

Characterisation of precursor and oxide powder

Thermal analysis (TG/DTA) was employed to examine the thermal stability of the precursor and its decomposition products. It follows from the TG and DTA curves, Fig. 1 that after the initial loss of water, the degradation of precursor completed in three stages. The first (I) stage, 180 to 240°C, shows a sharp mass loss of precursor. This sudden decomposition is attributed to the formation of NH_4NO_3. The second (II) stage, 240 to 440°C, shows a further mass loss of precursor which refers to decomposition of carbonates. The final (III) stage, 440 to 470°C, is associated with a large exothermic peak that could be caused by a combination of the decomposition of $Pb(NO_3)_2$ [16] according to the following chemical equation

$$2Pb(NO_3)_2 \xrightarrow{470℃} 2PbO+O_{2(g)}+4NO_{2\ (g)}$$

and the crystallisation of the phases from the amorphous precursor.

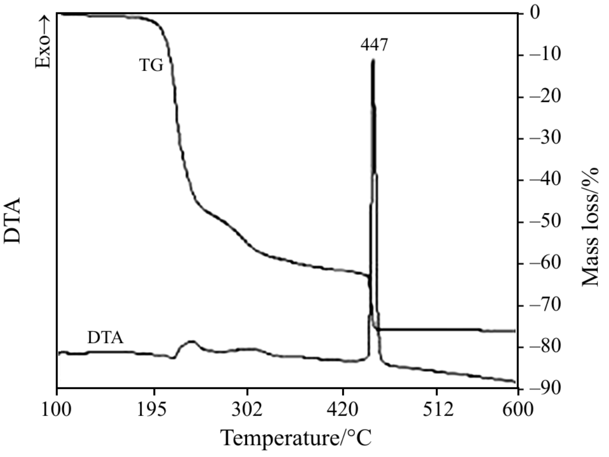

Fig. 1 TG and DTA curves for EDTA precursor

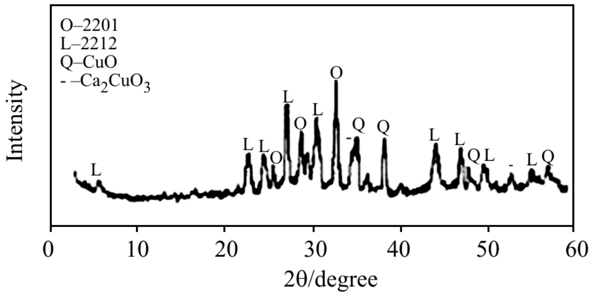

Fig. 2 X-ray diffraction patterns of precursor heated at 800°C

Figure 2 shows the XRD result for the product obtained by heating the material at 800°C. It is evident from the X-ray diffraction patterns that the 2212 phase is dominant in the sample. The thermal analysis was conducted for the sample calcined at 800°C to find out the optimum sintering temperature. Figure 3 shows two endothermic peaks for the sample at temperature of 855 and 870°C. The first endothermic peak, which occurred at temperatures between 835 and 865°C is associated with the partial melting. The second endothermic peak appeared at temperatures between 865 and 885°C. According to the Wong *et al.* [17, 18], 870°C is the decomposition temperature of the 2212 phase which disintegrates into $Bi_2Sr_2CuO_x$ (2201) and other Ca and Cu compounds and so it implies that the second endothermic peak is ascribed to this decomposition. The DTA data shows that with the addition of Pb, the partial melting peak of the material decreases as compared to Pb-free sample [19].

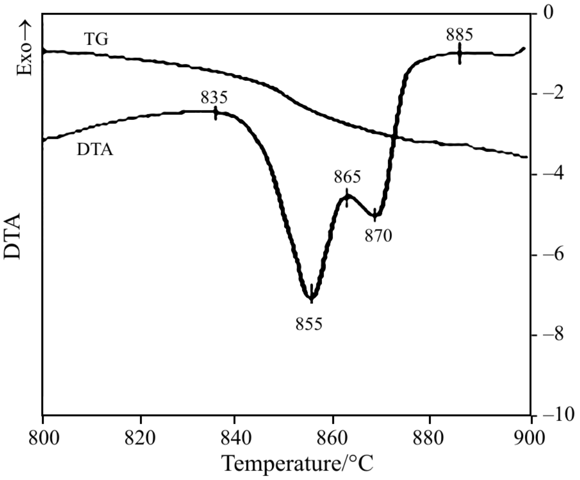

Fig. 3 TG and DTA curves for powder calcined at 800°C

Characterisation of sintered products

Figure 4 shows the XRD pattern of the samples sintered at 845°C for 48, 60 and 120 h. The 2223 phase, which had appeared in small amounts after 48 h increased with further heat treatment time (60 h) accompanied by a decrease in the amounts of 2212 phase and 2201 phase. Further increase in time (120 h) increased the amount of the 2223 phase. It is evident that the volume-fraction of the 2223 phase increases with time since its mechanism of production is a diffusional time-dependent process. If need arises

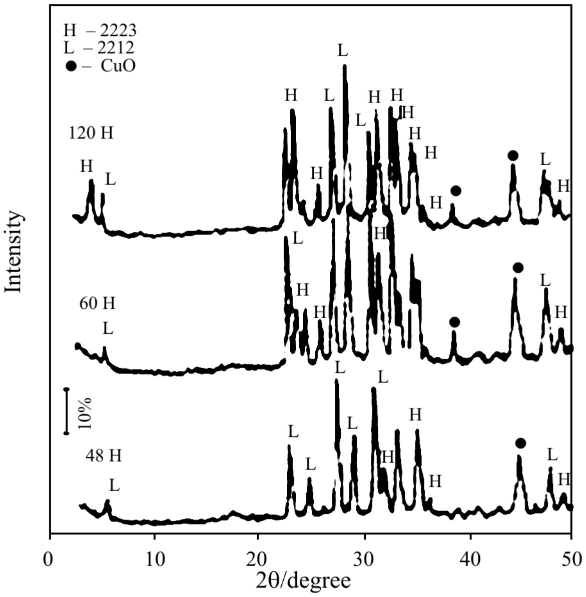

Fig. 4 X-ray diffraction patterns of sample sintered at 845°C for 48, 60 and 120 h

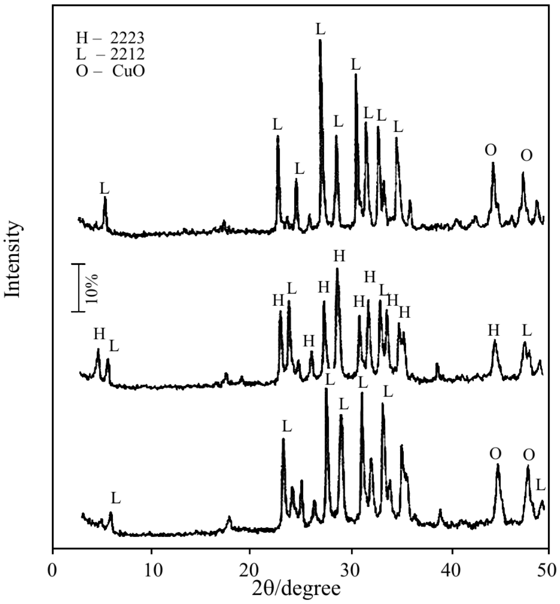

Fig. 5 X-ray diffraction patterns of sample sintered at 855°C for 6, 24 and 48 h

to develop the materials for commercial purposes, it is apparent that the sintering time of 5 days (120 h) is a long period to enhance the volume-fraction of the 2223 phase. However, sintering time period can be reduced by controlling the other factors, such as starting composition [20] and sintering the material in the partial melting region.

As indicated above, the 2223 phase was observed at 845°C after 48 h and its volume-fraction increased after 120 h heat treatment. At this temperature the sample also contained 2212 phase and CuO as shown by XRD results, Fig. 4, on the basis of these observations, it was planned to increase the sintering temperature so the pellets were sintered at 855°C which is the peak temperature as shown in Fig. 3. A high volume-fraction of the 2223 phase was observed in the sample sintered at 855°C for 24 h. Figure 5 shows the X-ray diffraction patterns of pellets sintered at 855°C for 6, 24 and 48 h. The characteristic peak (002) of 2212 and 2223 phases was only identified in the sample sintered at 855°C for 24 h. However, the characteristic peak of the 2223 phase increased with increase in time from 6 to 24 h and then decreased after 48 h. From Fig. 5, it follows that the major phase in the sample sintered at 855°C for 24 h is the 2223 phase. Small numbers of peaks of the phase 2223 were also observed in the sample sintered at 855°C for 6 h. However, the peaks of the phase 2223 were absent in the sample sintered at 855°C for 48 h. This may be due to the loss of oxygen during heating. It is known [11] that sintering the sample at high temperature for long duration is responsible for an oxygen loss of the sample resulting in the formation of CuO and 2212 phase as revealed by XRD patterns, Fig. 5. The volume- fraction of the 2223 phase relative to 2212 phase in the sample sintered at 855°C for 24 h was determined by XRD using the ratio $I_{h(002)}/(I_{h(002)l}+I_{l(002)})$. The $I_{h(002)}$ (25%) and $I_{l(002)}$ (11%) are the intensity values of the (002) peaks of the 2223 and 2212 phases, respectively as given in Fig. 5. Based on the analysis, a high volume-fraction of about 70% of the 2223 phase was noticed after holding at 855°C for 24 h.

Figures 6a–c show the SEM micrographs of the fractured surfaces of the samples sintered at 845°C for 60 and 120 h and at 855°C for 24 h. The figures show the plate-like grains in all the samples. The EDX analysis identified the high volume fraction of the 2223 phase in the sample sintered at 855°C for 24 h.

The presence of superconducting phases was also confirmed by VSM. Figure 7 shows the AC magnetic susceptibility of the samples sintered at 845°C for 48, 60 and 120 h. In the sample sintered for 48 h (curve a), the dominant superconducting phase is 2212. However, the volume-fraction of the 2223 phase increases, whereas the amount of the 2212 phase decreases with the increasing sintering time up to 60 h (curve b). In the sample sintered at 845°C for 120 h, again the dominant phase is 2212. However, the 2201 phase reduced to lower level as shown by the XRD results. Figure 8 shows the VSM results of the sample sintered at 855°C for 6 and 24 h. The curve a shows the multiphase (2212 and 2223) nature of sample sintered at 855°C for 6 h. The curve b in Fig. 8 clearly shows that the main phase is the 2223 phase with the T_C onset 113 K in the sample sintered at 855°C for 24 h. These results are in good agreement with the XRD results, Figs 4 and 5.

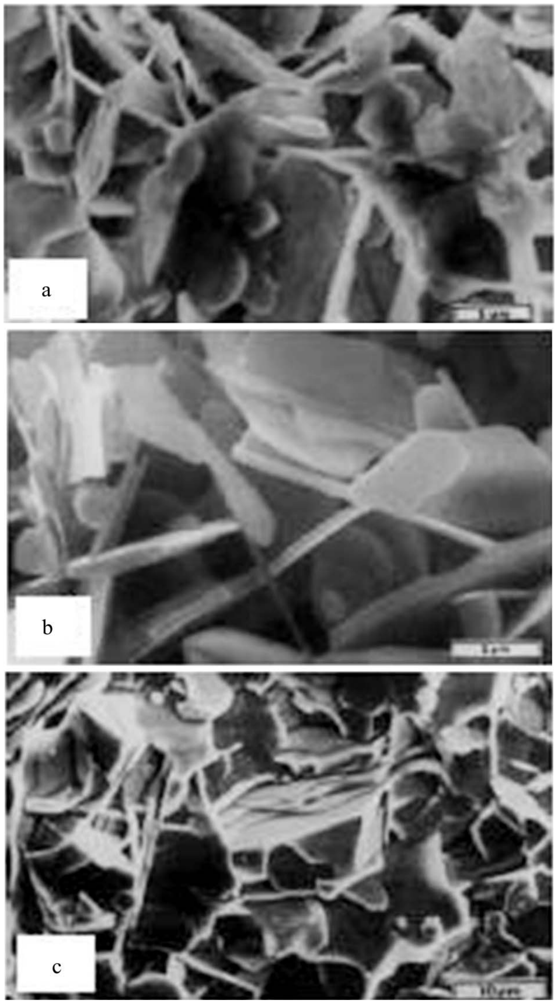

Fig. 6 SEM micrograph of the samples sintered at 845°C for a – 60 h, b – 120 h and c – at 855°C for 24 h

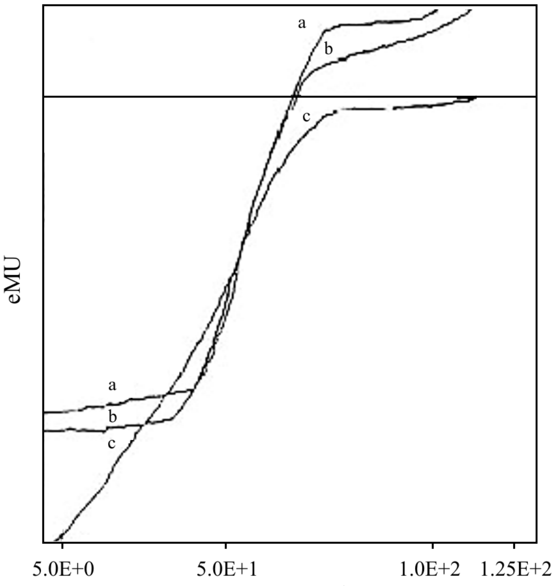

Fig. 7 VSM of samples sintered at 845°C for a – 48h b – 60 h and c – 120 h

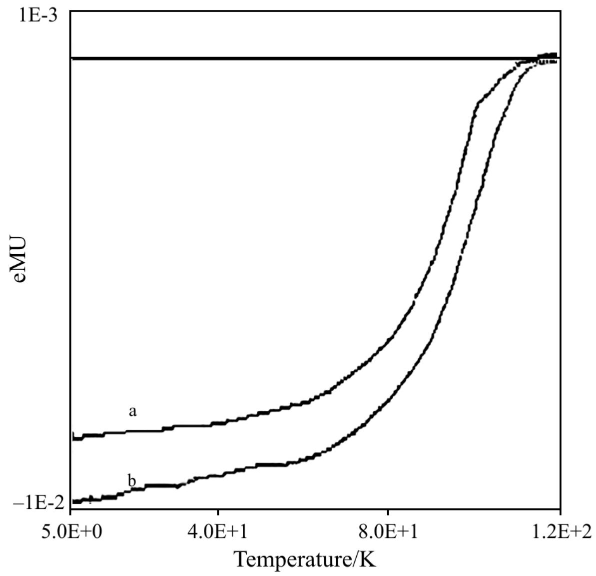

Fig. 8 VSM of samples sintered at 855°C for a – 6 h and b – 24 h

Conclusions

- The volume-fraction of the 2223 phase increases with time, the maximum volume fraction of the 2223 phase was obtained at 845°C for 120 h.
- A high volume-fraction of the 2223 phase was obtained in the sample at 855°C for 24 h.
- It was found that the formation of the high T_C phase was remarkably enhanced at the temperature of the endothermic peak.
- The 2223 phase is stable phase up to 855°C above which it is decomposed into 2212 and other phases.

Acknowledgements

The authors would like to thank the PINSTECH, Nilore, Islamabad for providing the opportunity to carry out this work. Thanks are also due to Gulzar Ali, Nadeem Ahmed, Saeed-ul-Hassan and Shahid Mahmood for their technical assistance.

References

1 B. Simendic and L. Radonjic, J. Therm. Anal. Cal., 79 (2005) 487.
2 A. H. Qureshi, M. Arshad, K. Masud and A. Saeed, J. Therm. Anal. Cal., 81 (2005) 363.
3 M. Picquart, T. Lopez, R. Gomez, E. Torres, A. Moreno and J. Garcia, J. Therm. Anal. Cal., 76 (2004) 755.
4 V. Balek, Z. Malek, J. Subrt, M. Guglielmi, P. Innozenzi, V. Rigato and G. Della Mea, J. Therm. Anal. Cal., 76 (2004) 43.

5 P. Staszczuk, D. Sternik and G. W. Chadzymski, J. Therm. Anal. Cal., 71 (2003) 173.

6 T. Ozawa, J. Therm. Anal. Cal., 72 (2003) 337.

7 R. Campostrini, M. Ischia and L. Palmisano, J. Therm. Anal. Cal., 71 (2003) 1011.

8 A. H.Qureshi, S. K. Durrani, M. Arshad, F. R. Sale, N. Arshad and S.U. Rehman, J. Chem. Soc. Pak., 25 (2003) 177.

9 Y. L. Chen and R. Stevens, J. Am. Ceram. Soc., 75 (1992) 1142.

10 D. Shi, M. S. Boley, J. G. Chen, M. Xu, K. Vandervoot, Y. X. Liao and A. Zangvil, Appl. Phys. Lett., 55 (1989) 699.

11 M. Pissas, D. Niarchos, C. Christides and M. Anagnostou, Supercond. Sci. Technol., 3 (1990) 128.

12 T. Hatano, K. Aota, H. Hattori, S. Ikeda, K. Nakamura and K. Ogawa, Cryogenics, 30 (1990) 611.

13 G. C. Tu, F. H. Chen and H. S. Koo, Supercond. Sci. Technol., 3 (1990) 134.

14 F. Chen, H. S. Koo and T. Y. Tseng, J. Am. Ceram. Soc., 75 (1992) 96.

15 A. Gholinia and F. R. Sale, J. Thermal Anal., 40 (1992) 349.

16 D. H. Williams and I. Fleming, Organic Chemistry, 4th Ed. McGraw Hill (1987).

17 W. Wong-NG, C. K. Chiang, S. W. Freeman, L. P. Cook and M. D. Hill, Am. Ceram. Soc. Bull., 71 (1992) 1261.

18 W. Wong-NG, C. K. Chiang, S. W. Freiman, P. C. Cook, N. M. Hwang and M. D. Hill, Materials Research Society Symposium Proceeding, 169 (1992) 123.

19 M. Rajabi and F. R. Sale, Eur. Ceramics Proceeding, 2 (1989) 2426.

20 D. Shi, M. Tang, M. S. Boley, M. Hash, K. Vandervoort, H. Claus and Y. N. Lwin, Phys., Rev. B: Condens. Matter, 40 (1989) 2247.

Received: July 27, 2005
Accepted: October 6, 2005

DOI: 10.1007/s10973-005-7233-3